Phytochemistry 145 (2018) 197–206

Contents lists available at ScienceDirect

Phytochemistry

journal homepage: www.elsevier.com/locate/phytochem

On the contributions of photorespiration and compartmentation to the contrasting intramolecular ^{2}H profiles of C_3 and C_4 plant sugars

Youping Zhou [a, b, f, *], Benli Zhang [a], Hilary Stuart-Williams [d], Kliti Grice [c], Charles H. Hocart [a, d], Arthur Gessler [b, e], Zachary E. Kayler [b, g], Graham D. Farquhar [d]

[a] School of Chemistry & Chemical Engineering, Shaanxi University of Science & Technology, Xi'an, China
[b] Institute for Landscape Biogeochemistry, ZALF, Germany
[c] WA-Organic and Isotope Geochemistry Centre, Department of Chemistry, Curtin University, Australia
[d] Research School of Biology, Australian National University, Australia
[e] Swiss Federal Institute for Forest, Snow and Landscape Research, Birmensdorf, Switzerland
[f] Leibniz Institute for Freshwater Ecology & Inland Fisheries, Germany
[g] USDA Forest Service, Northern Research Station, Lawrence Livermore National Laboratory, Livermore, CA 94550, USA

ARTICLE INFO

Article history:
Received 28 October 2017
Accepted 3 November 2017
Available online 28 November 2017

Keywords:
Sugar biosynthesis
Intramolecular ^{2}H distribution
Isotope effect
C_3 photorespiration
C_4 compartmentation

ABSTRACT

Compartmentation of C_4 photosynthetic biochemistry into bundle sheath (BS) and mesophyll (M) cells, and photorespiration in C_3 plants is predicted to have hydrogen isotopic consequences for metabolites at both molecular and site-specific levels. Molecular-level evidence was recently reported (Zhou et al., 2016), but evidence at the site-specific level is still lacking. We propose that such evidence exists in the contrasting ^{2}H distribution profiles of glucose samples from naturally grown C_3, C_4 and CAM plants: photorespiration contributes to the relative ^{2}H enrichment in H^5 and relative ^{2}H depletion in H^1 & H^6 (the average of the two pro-chiral Hs and in particular $H^{6,\ pro\text{-}R}$) in C_3 glucose, while ^{2}H-enriched C_3 mesophyll cellular (chloroplastic) water most likely contributes to the enrichment at H^4; export of (transferable hydrogen atoms of) NADPH from C_4 mesophyll cells to bundle sheath cells (via the malate shuttle) and incorporation of ^{2}H-relatively unenriched BS cellular water contribute to the relative depletion of H^4 & H^5 respectively; shuttling of triose-phosphates (PGA: phosphoglycerate dand DHAP: dihydroacetone phosphate) between C_4 bundle sheath and mesophyll cells contributes to the relative enrichment in H^1 & H^6 (in particular $H^{6,\ pro\text{-}R}$) in C_4 glucose.

1. Introduction

The stable hydrogen isotopic ratio ($^{2}H/^{1}H$) of carbon-bound hydrogen (C-H) of naturally synthesized plant carbohydrates (and other molecules such as lipids) has the potential to provide retrospective information about plant physiology, metabolism and climate (Luo and Sternberg, 1991; Luo et al., 1991; Martin and Martin, 1991; Yakir, 1992; Gleixner and schmidt, 1997; Sessions et al., 1999; Billault et al., 2001; Grice et al., 2008; Robins et al., 2003; 2008; Zhang et al., 2009; Zhou et al., 2010, 2011; 2015, 2016; Ehlers et al., 2015). Notably the $^{2}H/^{1}H$ in natural archives such as tree ring cellulose (Liu et al., 2015) or plant waxes in sediments (Niedermeyer et al., 2016) allows the reconstruction of long-term climate patterns and its impact on plant function. The full potential of such applications however has not been realized as photosynthetic and biosynthetic pathway-specific differences in $^{2}H/^{1}H$ (and $^{13}C/^{12}C$) are not necessarily evident at the molecular level and thus only part of the physiological and/or climate related signal can be extracted. Instead it is more evident at a site-specific level (Gleixner and Schmidt, 1997; Schmidt et al., 2003).

To realize such potential, the first step is to develop an analytical method that can access the site-specific $^{2}H/^{1}H$ ratios within a single carbohydrate molecule. Taking advantage of an NMR-based technique (^{2}H-SNIF-NMR: site-specific natural hydrogen isotopic fractionation studied by nuclear magnetic resonance) pioneered at the Université de Nantes in the early 1980s (Martin and Martin, 1981), Zhang et al. (1994) first obtained data showing that intramolecular ^{2}H profiles of C_3 and C_4 (endosperm starch) glucose are different. Later work by the same group, as well as from Schleucher and

* Corresponding author. School of Chemistry & Chemical Engineering, Shaanxi University of Science & Technology, Xi'an, China.
E-mail address: youping.zhou@sust.edu.cn (Y. Zhou).

https://doi.org/10.1016/j.phytochem.2017.11.004
0031-9422/

coworkers at Umeå University, confirmed such C_3-C_4 differences exist also in soluble sugars (including fructose), leaf starch and cellulose (Schleucher, 1998; Schleucher et al., 1998, 1999; Zhang et al., 2002; Betson et al., 2006; Augusti et al., 2006, 2007). From the illuminating work of these two groups, it was clear that ***i***) the intramolecular distributions of ^2H are non-random for both C_3 and C_4 plant glucoses; ***ii***) the H^1 and H^6 (the average of the pro-chiral Hs, and in particular $H^{6,\ pro\text{-}R}$) of C_4 glucose are always enriched, while H^4 and H^5 are always depleted in ^2H relative to the average of all 7 C-Hs (see Fig. 1 for glucose structure and the numbering of C-H atoms). In C_3 plant glucose, the profile is the opposite: H^1 & H^6 (and in particular $H^{6,\ pro\text{-}R}$) are always depleted, while H^4 & H^5 are always enriched in ^2H relative to the average of all 7 C-Hs. Notwithstanding these revealing intramolecular measurements, little effort has been made so far to explain what is causing such intramolecular ^2H profile differences between C_3 and C_4 glucoses. Valuable metabolic and photosynthetic information hidden in those profiles is thus not released but would be crucial for the full exploitation of physiological and environmental signals in natural archives.

In a recent effort made by Zhou et al. (2016) to provide a biochemical explanation for the molecular level C_3 *versus* C_4 ^2H differences of C-H in lipids synthesized via three independent pathways (fatty lipids via the acetogenic (ACT) pathway, phytol via the 1-deoxy-D-xylulose 5-phosphate (DXP) pathway and sterols via the mevalonic acid (MVA) pathway), it was suggested that pyruvate, the common precursor (for the three pathways) and NADPH used for lipid biosynthesis in C_4 plants have different isotopic compositions from those in C_3 plants due to photorespiration in C_3 and compartmentation of water (the primary hydrogen source) in C_4 plants. As lipid biosynthesis and carbohydrate metabolism in leaves are interrelated by triose phosphates, it is reasonable to assume that the biochemical mechanisms behind the molecular level differences between C_3 and C_4 lipids may also be evident in the intramolecular (positional level) ^2H distribution difference between C_3 and C_4 carbohydrates.

Providing a reasonable (and quantitative) biochemical explanation for the intramolecular ^2H profile of carbohydrate is a big challenge as there are many steps where H isotope effects can occur due to bond cleavage and formation, isotope exchange between and among metabolic intermediates and solvents (H_2O) and metabolic branching (Schmidt et al., 2003). In this VIEWPOINT, we have made the first attempt to rationalise the contrasting intramolecular profiles and by laying out a tentative framework, we hope to encourage others to fill in gaps or modify areas of ambiguity.

We propose that photorespiration and compartmentation contribute to the observed C_3 *versus* C_4 differences in glucose intramolecular ^2H profiles. We specifically describe 1) the likely mechanisms behind the relative enrichment of H^4 and H^5 in C_3 plant and relative depletion in C_4 plants, 2) the isotopic differences between C_3 and C_4 glucoses in H^1 and H^6, and lastly, 3) discuss the ^2H distribution in C_3 glucose as affected by growth.

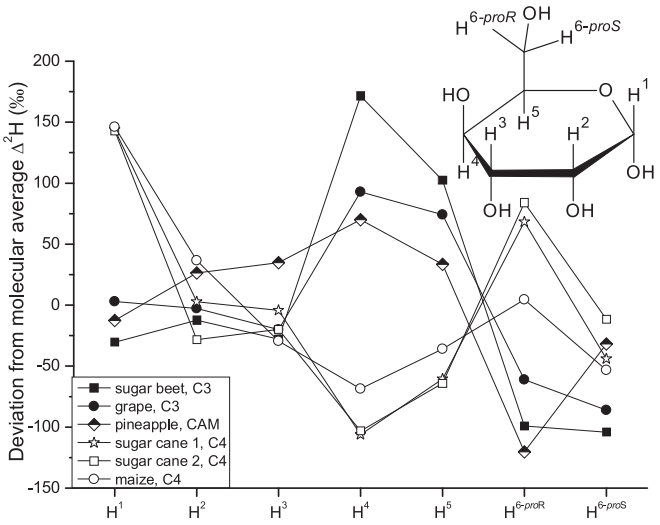

Fig. 1. Intramolecular ^2H distribution of glucose in fruit of C_3 (sugar beet and grape) and CAM (pineapple), and C_4 (sugarcane and maize, both NADP-ME) plants using the data of Zhang et al. (2002). The original $^2H/^1H$ data (in ppm) were converted to δ^2H using δ^2H (‰) = $[[(^2H/^1H)_{sample}-(^2H/^1H)_{SMOW}]/(^2H/^1H)_{SMOW}]$*1000, where $(^2H/^1H)_{SMOW}$ is 156 ppm and are expressed as deviation (Δ^2H) from the average of all 7 C-Hs (carbon-bound hydrogen atoms) in glucose. Similar profiles for leaf sugars, starch and stem carbohydrates were also reported by Schleucher (1998), Schleucher et al. (1999), Augusti et al. (2006), Betson et al. (2006), Augusti (2007, PhD thesis), and Augusti et al. (2008).

2. Relative ^2H enrichment at H^4 & H^5 in C_3 glucose

Since there is no reason to believe that the biochemistry of C_4 CBB (Calvin-Benson-Bassham) cycle leading to the synthesis of glucose is different from that in a C_3 cell, it is reasonable to assume that there are no step-specific differences in the isotope effects associated with the biochemical reactions between a C_3 cell and a C_4 cell (regardless of the cell types). From this assumption, it follows that position-specific isotopic differences between C_3 and C_4 glucose will be determined by the isotopic compositions of cellular water in which the biochemistries occur, the NADPH involved in reduction and the isotopic effects associated with their incorporation into and "shuttling" among the positions to which the H atoms (in question) are covalently attached.

Enrichment of H^4: when the two PGA molecules (**2a** and **2b**, the former is usually referred to as the "upper" PGA and the latter the "lower" PGA in most of the RubisCO biochemistry) generated at the first (carboxylation) step of the CBB cycle (Fig. 2) is converted to GAP (**4a**) under the catalysis of GAPDH, a H^- from the chloroplastic NADPH is introduced into the H^1 of GAP (**4a**). As the NADPH -derived H is known to be highly depleted in ^2H (Luo et al., 1991) and that the donation of an H^- is predicted to have a large kinetic isotope effect KIE (Miller and Hinck, 2001), the H^1 of GAP (**4a**) (H^4 of glucose) should therefore be even more depleted relative to the chloroplastic NADPH transferable hydrogen. This is, however, contrary to the observation that H^4 is most enriched in C_3 glucose (Fig. 1 and **8a**, **8b**, **9a**, **9b,** starch and sucrose in Fig. 2). We provide below two mechanisms to account for the apparent enrichment at H^4: ***i***) during the conversion of H^2 of GAP (**4a**) to $H^{1,\ pro\text{-}R}$ of DHAP (**5a**), H of cellular (chloroplastic) water (H_2O) is also introduced (in the form of a proton H^+) into DHAP (**5a**) and presumably also into H^1 of GAP (**4a**) (O'Donoghue et al., 2005a,b; Pionnier and Zhang, 2002; Pionnier et al., 2003, Fig. 3), the isotopically relatively enriched cellular water passes on the enrichment to H^1 of GAP (**4a**) and H^4 of glucose (**9a**); ***ii***) as suggested by Tcherkez (2010), an EIE (equilibrium isotope effect) of TPI which enriches H^1 of DHAP (**5a**), may also contribute to the enrichment at H^1 of GAP (**4a**) (H^4 of glucose). Of the two possible mechanisms, we rank the first one more likely as it not only accounts for the H^4 enrichment in C_3 glucose but also explains in part the H^4 depletion in C_4 glucose (see the next section). The ^2H-enriched cellular (chloroplastic) water alone, or in combination with the EIE-caused enrichment, more than compensates for the depletion due to the introduction of ^2H-depleted (transferable H of) NADPH to H^1 of GAP (**4a**).

We also argue that the enrichment of H^5, which comes from H^2 of GAP (**4a**) is a result of photorespiration in C_3 cells. First, the transferable hydrogen in NADH in the peroxisome is enriched in ^2H due to transhydrogenation to form NADPH (see Fig. 2-the

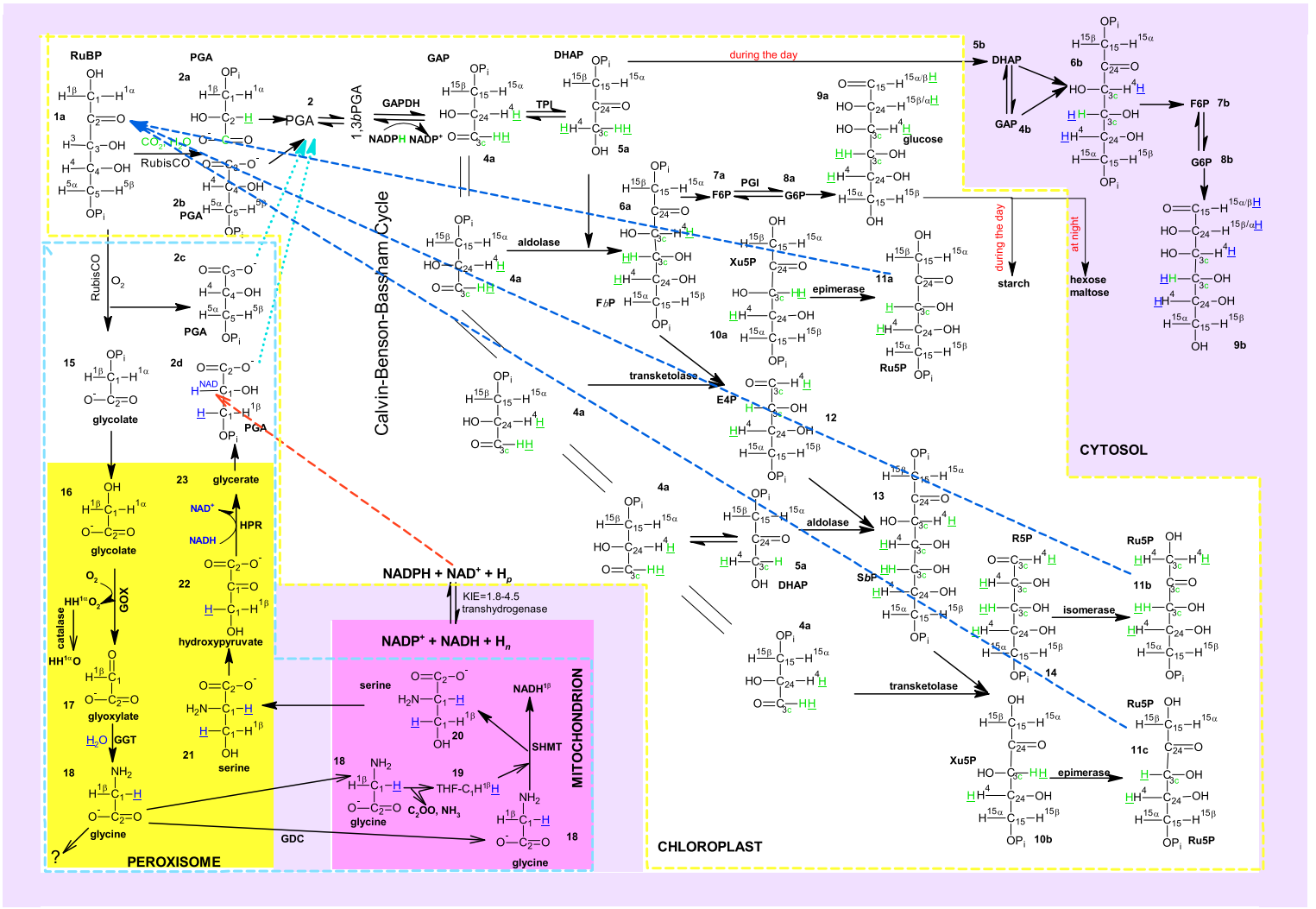

Fig. 2. Metabolic relationship between the Calvin-Benson-Basham (CBB) Cycle and photorespiration in relation to the movement of H-atoms in a typical C_3 mesophyll cell. Colour-coding is used to distinguish different cellular compartments: white: stroma of chloroplast; pink: cytosol; red: mitochondrion; yellow: peroxisome; $\underline{H}_2O$: (chloroplastic) stromal water. $\underline{H}_2O$: cytosolic water; Photorespiration which spans the chloroplastic stroma, cytosol, peroxisome and mitochondrion is enclosed in the blue dashed box; CBB Cycle is enclosed in the bright yellow dotted polygon. For clarity, biochemical steps (and enzymes involved in those steps) where no hydrogen or hydrogen isotope effect is involved were omitted from illustration. **19**: THF-$C_1H^{1\beta}\underline{H}$: tetrahydrofolate-$C_1H^{1\beta}\underline{H}$. Abbreviations are: GOX: glycolate oxidase (Dellero et al., 2015); GGT: glutamate-glyoxylate transaminase (Jordan and Akhtar, 1970); HPR: hydroxypyruvate reductase; GDC: glycine decarboxylase complex; SHMT: serine hydroxymethyltransferase: glyoxylate aminotransferase (Shirch and Jenkins, 1964). C-atoms in RuBP (**1a**) are numbered following organic chemistry convention while H-atoms of RuBP (1a) take the numberings of the C-atoms they are attached to. For example, $H^{1\alpha}$ refers to one of the two H-atoms attached to C_1 of RuBP (**1a**). Any compounds derived from RuBP have their C and H numbered in a way that can be traced back to RuBP (**1a**). For example, in GAP (**4a**) in Fig. 2, C_{15} means that this C has equal contributions from C_1 and C_5 of RuBP (**1a**), while the H connected to C_{24} (written as $\underline{H}H^4$) means that it has a (but not necessarily an equal) contribution from $\underline{H}$ and H^4 in the original RuBP (**1a**). The C_{3C}, C_{24}, and C_{15} in GAP (**4a**) and DHAP (**5a**) are structurally equivalent to the C1, C2 and C3 in GAP (**4f-5i**) and DHAP (**5g-5j**) in Fig. 3 respectively. α and β refer to the *pro*-R and *pro*-S positions, respectively, in all compounds (Hanson, 1984). The conversion of glycine (**18**) to serine (**20**) in Fig. 2 involves first the decarboxylation of glycine to give NH_3, CO_2, NADH and a $-CH_2-$ unit temporarily captured by THF (tetrahydrofolate) under the catalysis of GDC: $\underline{\text{glycine} + \text{NAD}^+ + \text{THF} \rightarrow N^5,N^{10}\text{-methylene-THF} + \text{NADH}^{1\beta} + \text{NH}_3 + \text{C}_2\text{OO}}$ and subsequent N^5,N^{10}-methylene-THF reaction with another molecule of glycine to give serine: $\underline{N^5,N^{10}\text{-methylene-THF} + \text{glycine} \rightarrow \text{serine} + \text{THF}}$ under the catalysis of GDC/SHMT complex. Although it is possible a small isotope effect is associated with the transfer of the $-CH_2-$ unit due to the complex nature of glycine metabolism involving equilibrium between different pools (methylene, formyl, methenyl) and exchange of folates between cellular compartments, it is explicitly assumed here that such IE is insignificant as the abstraction of the pro-R (the $\underline{H}$) from one of two glycine (**18** of Fig. 2) molecules by GDC (glycine decarboxylase complex) and the capture of the $-CH_2-$ unit by SHMT to form serine is highly likely to be effected in a concerted fashion, such that the $-CH_2-$ unit released from the glycine is used in its entirety for serine synthesis. This figure, and the rules governing labelling of compounds and numbering of C and H atoms are essentially the same as those in the Fig. 2 of Zhou et al. (2016). (For interpretation of the references to colour in this figure legend, the reader is referred to the web version of this article.)

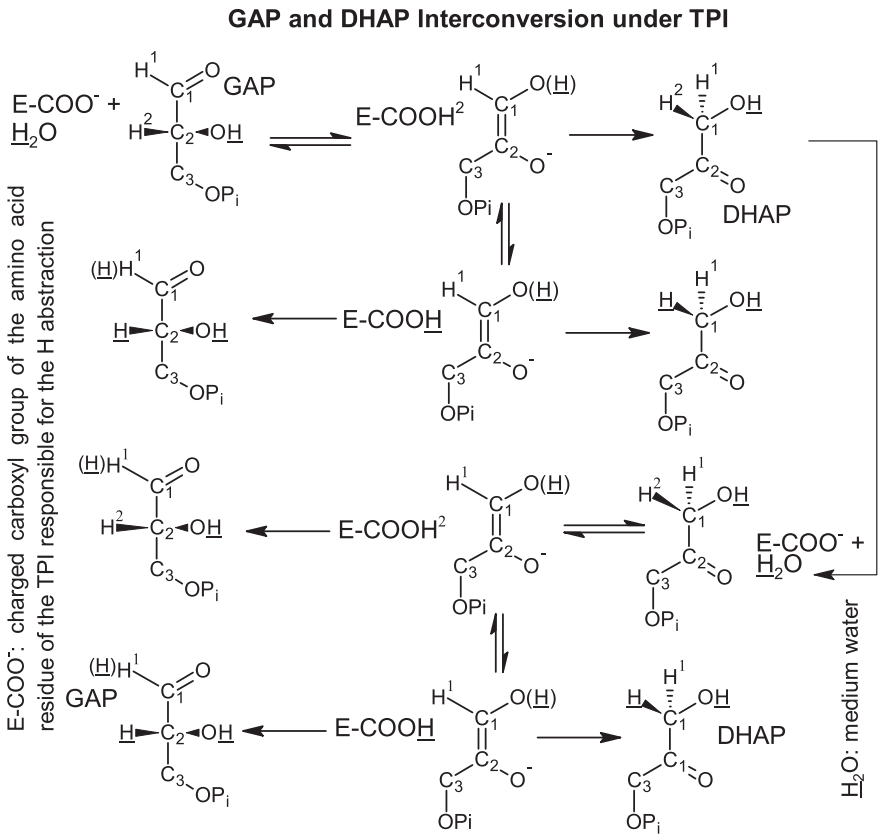

Fig. 3. DHAP↔GAP interconversion by TPI (triose phosphate isomerase) showing the movement of relevant H-atoms according to O'Donoghue et al. (2005a,b), Pionnier & Zhang (2002), Pionnier et al. (2003). At equilibrium, H-atoms at C1 and C2 of DHAP and GAP have a mixed source from H-atoms originally at C1, C2 and the water medium. E-COO⁻ is the charged carboxyl group of the amino acid residue responsible for the abstraction of H. Note that the numbering of carbons in this scheme follows organic chemistry convention. The C1, C2 and C3 are structurally equivalent to C_{3C}, C_{24}, and C_{15} in GAP (**4a**) and DHAP (5**a**) in Fig. 2 respectively.

interconversion between NADH and NADPH; Keister et al., 1960; Bizouarn et al., 1995; baz Jackson et al., 1999; Zhang et al., 2009; Zhou et al., 2016; the transhydrogenase activity occurs across the outer membrane of the mitochondrion where the NADH is converted to NADPH with a KIE of as high as 5.8, leaving the residual NADH enriched in ^{2}H). Under normal conditions when the average RubisCO oxygenation/carboxylation ratio is around 1/3 (1/4 to 1/2 according to Heldt (2005)), the photorespiration generated-**PGA** (**2d**) contributes 1/14 of the total H in the chloroplastic PGA (**2** in Fig. 2) that ends up at C4 of glucose. A KIE of 3.10 is high enough to be able to account in full the average difference of 150‰ between the most enriched and most depleted positions in glucose (Fig. 1). Second, during the generation of PGA (**2d**) from hydroxypyruvate (**22**) in the peroxisome, the transferable hydrogen from NADH (H^{NAD}) is introduced into the C2 of PGA (**2d**). The H^{NAD} contributes directly to the H^5 of glucose (8**a**, **9a** and starch in Fig. 2). Last, when GAP (**4a**) is condensed with DHAP (**5a)** by aldolase to produce F*b*P (**6a**), the enrichment signal at C2 of GAP (**4a**) ends up in H^5 of F*b*P (**6a**). The GAP (**4a**) ↔DHAP (**5a**) interconversion should theoretically (O'Donoghue et al., 2005a,b; Tcherkez, 2010) also enrich the H^1 of DHAP (**5a**, therefore H^3 of F*b*P **6a**), however the enrichment at H^1 of DHAP (**5a**) and concomitantly at H^3 of F*b*P (**6a**) is partially cancelled out by the KIE ($k_H/k_D = 4$) associated with TPI (Fig. 3) as suggested by Tcherkez (2010).

Another possibility is that if the H^4 (H^4 of RuBP (**1a**)) of carboxylation-generated PGA (**2b**) is more enriched in ^{2}H than that of the corresponding position in PGA (**2a**) (the green underlined H, from chloroplastic H_2O, Fig. 2), then contribution to the chloroplastic PGA (**2**) pool from oxygenation-generated PGA (**2c**) (isotopically identical to PGA (**2b**) at position-specific level) should enrich H^2 of the chloroplastic PGA pool (**2**) and subsequently H^5 of G6P (**8a**). However, this is unlikely because H^4 of RuBP (**1a)** is unlikely to be more enriched than chloroplastic (stromal) H_2O and the H of PGA (**2a**) should be isotopically close to that of H_2O because the isotope effect associated with its incorporation into PGA (**2a**) is negligible (Kawashima and Mitake, 1969; Siegel et al., 1972) and that chloroplastic H_2O is highly enriched relative to organically-bound H due to leaf water evaporative enrichment. The overall isotope effect associated with the incorporation of chloroplastic water H_2O into C2 of RuBP (**1a**) as implied by Tcherkez et al. (2013) can only be small as otherwise the isotopic composition of RuBP (**1a**) would not be steady under steady state. Therefore enrichment at C5 of glucose cannot be due to isotopic difference at C2 between PGA (**2a**) and PGA (**2b**), implying that NADH is still the most likely source of enrichment at C5 in C_3 plant glucose (**9a**).

3. Relative ^{2}H depletion at H^4 & H^5 in C_4 glucose

In C_4 plants, photorespiration is largely suppressed due to the highly efficient bundle sheath CO_2-concentrating mechanism (CCM). Thus there is minimal contribution of ^{2}H-enriched transferable hydrogens from NADH to the PGA (**2e**) pool in the bundle sheath chloroplast and, therefore, there is no enrichment of H^5 relative to other sites within the C_4 glucose. This, however, still cannot explain why H^4 and H^5 are relatively depleted in ^{2}H, when compared to other intramolecular positions. It is, therefore proposed that depletion is due to the export of ^{2}H-depleted (transferable hydrogen of) NADPH (via the malate shuttle) from the M

cells to the BS cells and the use of unenriched or slightly enriched BS cellular water for glucose biosynthesis.

The initial fixation of CO_2 into OAA (oxaloacetate, **25a**) in the cytosol of M cells by PEPC (phospho*enol*pyruvate carboxylase) is spatially separated from final fixation by RuBP carboxylase in the BS cells (Fig. 4A). Unlike C_3 chloroplasts, which possess both PS II & PS I (photosynthesis systems II & I), the BS chloroplasts in NADP-ME (NADP malic enzyme) plants have only PS I and therefore limited ability to generate NADPH. Consequently, reducing power needs to be imported from M cells via the malate (**26a**)-pyruvate (**27a**) shuttle (to generate NADPH from within the BS). This importation involves first reduction of OAA (**25a**) to malate (**26a**) by NADPH catalysed by NADP-MDH (NADP Malate Dehydrogenase) in the M cells and then decarboxylation/reduction by NADP-ME (NADP Malic Enzyme) to release CO_2 and NADPH in the BS cells. Due to the high KIE associated with reduction of OAA (**25a**) to malate (**26a**) (Hermes et al., 1982; Grissom and Cleland, 1985), the exported hydrogen (the H^s in malates (**26a**) used to make NADPH (the $NADPH^s$ formed during conversion of **26a** to **27a**) under the catalysis of NADP-ME in the BS chloroplast is expected to be depleted in ^2H relative to the residual (hydrogen of) NADPH ($NADPH^r$) in the M cell chloroplast (the relatively ^2H-enriched residual (hydrogen of) NADPH in the M chloroplast is used for synthesis of phytol and possibly other reduction processes; see Zhou et al. (2016) for further explanation). Although NADP-ME has a capacity to introduce a further depletion to the H^s in the BS $NADPH^s$ with a modest KIE of 1.17 (Cook et al., 1980), such depletion can be treated as insignificant as it can be reasonably assumed that malate (and the H^s it carries over to the BS) is converted to pyruvate in its entirety.

When PGA (**2e**) is reduced by the imported ^2H-depleted $NADPH^s$ in the BS to GAP (**4d**) or by the same H^s to GAP (**4c**) in the M, the depletion signal of $NADPH^s$ and further depletion as a result of KIE of 5–5.5 (Canellas and Cleland, 1991), is passed onto GAP (**4c** and **4d**). Note that the portion of H^s that ends up in GAP (**4c**) (and **5c**) is likely to be enriched relative to the portion of H^s that is used to reduce **OAA** (**25a**), but it is still depleted relative to H^m as GAP (**4c**) is upstream of the steps where residual NADPH ($NADPH^r$) is used for reduction for (downstream) metabolic events. In a properly functioning C_4 cell, it is reasonable to assume that priority is given to the malate-pyruvate shuttle, then to the CBB cycle and finally to downstream reactions where NADPH is needed. On reaching isotopic equilibrium between GAP (**4c** and **4d**) and DHAP (**5c** and **5d**) under the catalysis of TPI in both BS and M cells, and when DHAP (**5d**) and GAP (**4d**) are condensed to make F*b*P (**6c**), the depletion signal is retained in F*b*P (**6c**) and passed onto the H^3 and H^4 of the hexoses F6P (**7c**), G6P (**8c**), starch and glucose (**9c**). Hence, the compartmentation of C_4 photosynthesis and the transfer of H from NADPH is most likely contributing to the observed H^4 depletion relative to other sites within the C_4 plant glucose. However, the depletion at H^3 MIGHT be diminished due to the H^3 acidity of fructose (note that the sugars used for position-specific H isotopic analysis by NMR at natural abundance were extracted from fruits in their free form rather than their phosphorylated form) in the alkaline BS cytosol (see Fig. 5).

The argument here for the ^2H-depletion associated with M-to-BS export of (transferable H of) NADPH is further strengthened by the fact that the CAM glucose intramolecular ^2H profile is very similar to that of C_3 rather than C_4 plants (Fig. 1). This is despite the biochemical similarity to C_4 plants in that CAM uses PEPC for initial fixation of CO_2 into OAA (**25a**), with final fixation of CO_2 via the CBB cycle (Heldt, 2005). Unlike C_4 plants, there is no spatial separation of photosynthetic CO_2 fixation or inter-cellular (M to BS) export of (transferable H of) NADPH in CAM plants (as both fixation of CO_2 and NADPH generation occur within a single cell, as in a C_3 cell). The export-associated NADPH depletion therefore does not exist in CAM plants which are found to exercise gluconeogenesis (Gilbert et al., 2012). Although PGA (**2e**) reduction (to DHAP **5c**) in the M cells can contribute to DHAP (**5d**) pool in the BS cells, such contribution (in NADP-ME subtype) is supposedly insignificant (and even smaller in NAD-ME and PCK subtypes as the BS cells of these two subtypes are competent in NADPH generation) than that in the BS. This is because 1) comparative proteomic studies by Majeran et al. (2005) convincingly showed that the enzymes for PGA reduction (GAPDH) and sugar synthesis are mainly found in the BS cells; 2) starch granules are mainly found in BS chloroplasts (Taiz and Zeiger, 2006) and 3) the rapid interconversion between DHAP (**5d**) and GAP (**4d**) would have replaced the M cellular H signal carried over by the DHAP (**5c**) in its entirety with BS cellular water H. The H^2 and H^3 relative enrichment in CAM glucose also lends support to the inference that DHAP (**5c**) in CAM plants is relatively ^2H-enriched when compared with C_3 plants as the cellular water of CAM plants is known to be more enriched than that of C_3 plants grown in close proximity (Sternberg et al., 1986).

As to the depletion of H^5 in C_4 glucose, since the exported (hydrogen of) NADPH does not exhibit itself at H^5 of glucose biosynthesized in the BS cells, and there are no differences in the biochemistries of glucose biosynthesis in C_3 M cells and C_4 BS cells, the most likely explanation is that BS cellular water in which sugar biosynthesis occurs is depleted (although still relatively enriched against organically-bound H) relatively to that of the M cells. Although we argue for a role of the isotopic difference in the cellular water available for glucose biosynthesis in shaping H^5 isotopic differences between C_3 and C_4 glucoses, we acknowledge that the former may not be able to account in full for the latter as Zhou et al. (2016) estimated that on average, M cellular water is 60‰ more enriched in ^2H than that of the BS.

4. H^1 & H^6 (in particular $H^{6,\ pro\text{-}R}$) depletion/enrichment in C_3/C_4 glucose

Based on Fig. 2 and the discussion above, it can be inferred that the two Hs ($H^{5\alpha}$, the *pro*-R H and $H^{5\beta}$, the *pro*-S H) at C5 of RuBP (**1a**) are replaced at a lower rate relative to the other four C-Hs in the CBB cycle (compare RuBP (**1a**) with the three regenerated Ru5Ps **11a**, **11b** and **11c** in Fig. 2). Although photorespiration-generated PGA (**2d**), when mixed with the chloroplastic PGA (**2**) pool, tends to enrich these two H^5s, such enrichment can be decreased significantly by the TPI & PGI-catalysed exchange opportunities with chloroplastic (stromal) water at other positions within C_3 plant glucose (**9a**, **9b**, starch and sucrose in Fig. 2). The $H^{6,\ pro\text{-}R}$ is relatively depleted (against other Hs) because this H has the lowest contribution (even more slowly exchanged than $H^{6,\ pro\text{-}S}$) from PGA (**2d**). Note that the two Hs at C3 of PGA (**2d**) have different origins: the H is from water and enriched due to evaporation while the $H^{1\beta}$ is inherited from $H^{1\beta}$ of RuBP (**1**). In C_4 plants, due to the inhibition of photorespiration there should not be a relative depletion at H^1 and H^6. Even so, the inhibition of photorespiration still cannot explain the observation that the C1 and C6 sites are the most enriched in C_4 glucose (**9c** and starch in Fig. 4A).

Related to the compartmentation of C_4 NADP-ME photosynthesis is the shuttling of triose-phosphates between BS and M cells (Fig. 4A). When PGA (**2e**) is exported to M cells, the two prochiral Hs at C3 are (indirectly) exchanged with M cellular water via the following mechanism: the PGA (**2e**) imported from the BS cells is converted to pyruvate (**27a**) via PGA (**2e**) →1,3*b*PG (**29**) →2PGA (**28**) →PEP (phosphoenolpyruvate, **24b**) →pyruvate (**27a**) according to von Caemmerer and Furbank (2016) (see Friso et al. (2010) and http://plantsinaction.science.uq.edu.au for the reconstructed metabolic pathway in the BS and M chloroplasts). This process introduces a H from M cellular water to the C3 of PGA (**2e**), with a

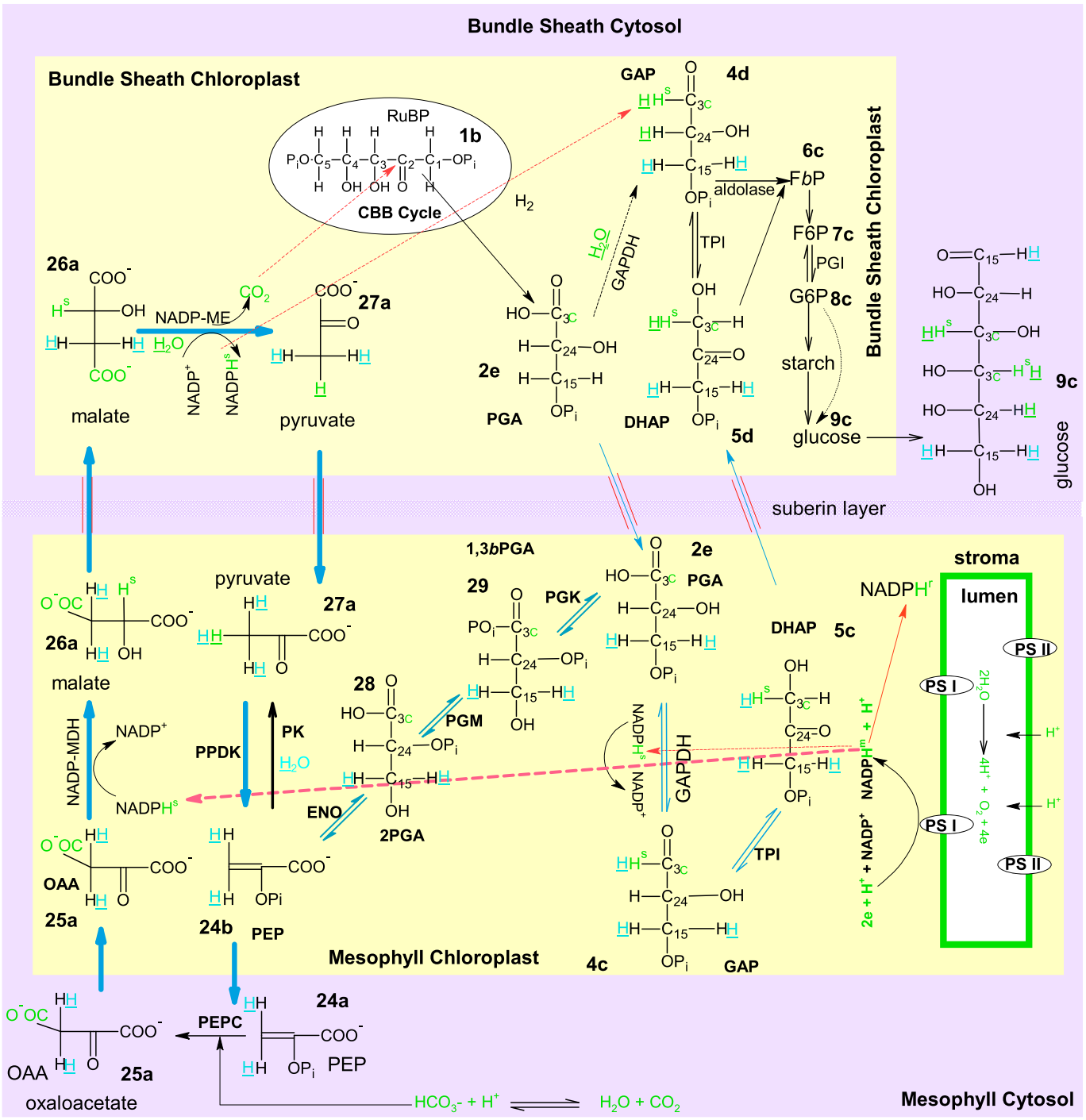

Fig. 4. A. Compartmentation of C_4 photosynthesis into mesophyll cell and bundle sheath cell in a typical C_4 NADP-ME plant. In this C_4 subtype, the malate (**26a**)-pyruvate (**27e**) shuttle is the dominant shuttle between the mesophyll and bundle sheath with a high flux indicated by a thick arrow. The PGA (**2e**)-DHAP (**4c**) shuttle form an integral part of the CBB Cycle in the bundle sheath cell. Comparative proteomics does show that GAPDH (the activity of which is indicated by the arrow between PGA (**2e**) and GAP (**4d**)), TPI and PGI (Majeran et al., 2005) are present in high content while reconstructed metabolic pathways from proteomics studies also show that glycolysis occurs in M chloroplast (Friso et al., 2010). Glycolysis links the malate-oxaloacetate shuttle and triose phosphates shuttle with PEP (phosphoenolpyruvate). Conversion of PEP (**24b**) to Pyruvate (**27a**) by PK (pyruvate kinase) and back to PEP (**24b**) by PPDK (phosphopyruvate dikinase) introduces M cellular water (^{2}H-enriched relative to BS cellular water) to GAP (**4c** and **4d**) and DHAP (**5c** and **5d**) via the glycolysis pathway. On condensing to make F*b*P (**6c**), the enrichment signature ends up in C1 and C6 of F6P (**6c**) and glucose (**9c**). NADPH produced in a mesophyll chloroplast ($NADPH^m$) is shuttled to a bundle sheath chloroplast to meet the high demand for reducing power in the bundle sheath chloroplast due to the absence of PS II. The consequence of this NADPH shuttle is that (the transferable H of) the residual NADPH ($NADPH^r$) in a mesophyll cell chloroplast is ^{2}H-enriched relative to its C_3 plant counterpart while the shuttled-over H ($NADPH^s$) is depleted as a result of a high KIE associated with NADP-ME (NADP malic enzyme) activity (Hermes et al., 1982; Grissom and Cleland, 1985). NADP-ME: NADP malic enzyme; OAA: oxaloacetate; PEPC: phospho*enol*pyruvate carboxylase; NADP-MDH: NADP malic dehydrogenase. TPI: triose phosphate isomerase. DHAP: dihydroxyacetone phosphate; GAP: glyceraldehyde phosphate; F6P: fructose-6-phosphate; G6P: glucose-6-phosphate; F*b*P: fructose-1,6-*bis*phosphate. The numbering and lettering of the C and H-atoms follow the rules described in Fig. 2. The H and H are from BS and M cellular (chloroplastic) waters respectively. This figure, and the rules governing the labeling of compounds and numbering of C and H atoms are essentially the same as those in the Fig. 3A of Zhou et al. (2016). Fig. 4B. Compartmentation of C_4 photosynthesis into mesophyll cell and bundle sheath cell in a typical C_4 NAD-ME plant (Edwards and Voznesenskaya, 2011; Edwards and Walker, 1983). In this C_4 subtype, the aspartate (**29**)-alanine (**28**) shuttle is the dominant shuttle between the mesophyll and bundle sheath; the PS II in the chloroplasts of both cell types are competent to generate NADPH, and therefore no NADPH is transported across the two cell types; no suberin lamella exists between mesophyll and bundle sheath cells that may restrict the flow of water between them. Reduction of OAA (**25b**) to malate (**26b**) occurs in bundle sheath mitochondria using NADH rather than NADPH. The enzyme NAD-ME is NAD malic enzyme. Other enzymes are the same as in Fig. 4A. The numbering and lettering of C and H also follow the rules described in Fig. 2. This figure, and the rules governing the labelling of compounds and numbering of C and H atoms are essentially the same as those in the Fig. 3B of Zhou et al. (2016).

slight KIE of 1.17 (Gold and Kessick, 1965), leading to a loss of prochiralities of the two Hs at C3 of PGA (**2e**). Since the three Hs at C3 of the thus-formed pyruvate (**27a**) are achiral, the M cellular water signal carried by the pyruvate (**27a**) is partially passed onto the PEP (**24b**). When PEP (**24b**) is converted back to GAP (**4c**) in the reverse reactions via PEP (**24b**) →2PGA (**28**) →1,3*b*PG (**29**) → PGA (**2e**) →GAP (**4c**), the M cellular water ends up in the C3 of GAP (**4c**, Pionnier and Zhang, 2002; see also Figure B-1-2 in the chapter B-I of the PhD thesis by Sébastian Pionnier; See Fig. 6 for the detailed mechanism for the labelling of the two C3 Hs of GAP). It can be assumed that M cellular water is enriched relative to that of BS as the latter is separated from the former by water impermeable suberin layers. Smith et al. (1991) gave indirect experimental evidence supporting our assumption as they showed that the parts of the leaf tissues containing BS cells were (in contrast to the M cells) only slightly subjected to evapotranspiration-caused isotopic enrichment. Zhou et al. (2016) estimated that on average M cellular water is approximately 60‰ more enriched than that of BS cells (see Tables 1 and 2 of Zhou et al.(2016)) based on the survey of over 30 species of C_3 and C_4 grasses in tropical Hainan. This water related enrichment signal is incorporated into the two H^3s of GAP (**4c**) and DHAP (**5c**) in mesophyll cells. When DHAP (**5c**) in mesophyll cells is shuttled back to the BS for sugar synthesis, such enrichment is incorporated at C1 and C6 of C_4 glucose (**9c** and starch in Fig. 4A). This is consistent with C_4 plant sterols (not shown here, see Zhou et al. (2016) for further information) being enriched relative to C_3 plant sterols as sterols inherit part of their hydrogen from C1 and C6 of glucose (even though H^4 and H^5 in C_4 plant glucose are depleted). Thus, it can be deduced that the enrichment of H^1 and H^6 of C_4 NADP-ME glucose (**9c** and starch in Fig. 4A) is best explained by the shuttling of triose-phosphate (DHAP, **5c**) between bundle sheath and mesophyll cells.

Although it can be argued that a similar enrichment at C1 and C6 (in particular the latter) can be expected for C_3 glucose as conversion from pyruvate to PEP by PPDK and back to pyruvate by PK also occurs in C_3 chloroplasts, the differences in pyruvate/PEP ratio and the PPDK activity between C_3 and C_4 M cells predict otherwise. The PPDK activity of C_4 M cell is much higher (>5.4 fold, Ishimaru et al., 1998) than that of C_3 and the pyruvate/PEP ratio for C_4 is much lower than that of C_3. The conversion of pyruvate to PEP by PPDK involves an abstraction of a C-H from the methyl group of pyruvate, the high KIE (4.25, Croteau and Wheeler, 1987) associated with the abstraction depletes ^2H of the methylene group of PEP. In C_4 cells, the conversion is high (Ishimaru et al., 1998) so that the methylene group in PEP should be isotopically close to the methyl group of pyruvate. In C_3 cells, the conversion is low, therefore the methylene group of PEP is very depleted in ^2H relative to the methyl group of pyruvate.

Since a similar mesophyll-*versus*-bundle sheath cellular water enrichment does not exist in typical NAD-ME species (see the discussion in Zhou et al., 2016), one might predict that a similar enrichment of H^1 and H^6 does not exist in NAD-ME (see Fig. 4B for the compartmentation of C_4 photosynthesis and the origins and histories of glucose C-Hs) soluble glucose. Unfortunately, there are currently no intramolecular ^2H data for NAD-ME soluble glucose that allow us to test this prediction. Although the intramolecular ^2H profile of glucose in cellulose of *Bouteloua gracilis*, a NAD-ME grass, does show similar enrichment at H^1 and H^6 (Augusti, 2007), the isotopic modifications from leaf soluble sugar to cellulose (structural carbohydrate) make it uncertain if *B. gracilis* cellulose is representative of NAD-ME soluble glucose. Even if it is, H^1 and H^6 enrichment may still exist as NAD-ME bundle sheath and mesophyll cellular waters are predicted to be relatively enriched against C_3 species. How this bundle sheath and mesophyll cellular water enrichment is reflected in the intramolecular profile of soluble glucose is determined by the fractional contributions of the two cell types to the synthesis of the soluble sugars. Surveying more C_4 subtype (and C_3) species for molecular and intramolecular isotope analysis should provide better insights into this issue.

5. Between-site ^2H distribution ratios with growth conditions in C_3 glucose

For C_3 plant glucose (**9a**, **9b**, starch and sucrose in Fig. 2), it was reported that when the $[O_2]/[CO_2]$ ratio (oxygenation over carboxylation ratio: V_o/V_c) increases, the ^2H distribution ratio $H^1/H^{6,pro\text{-}R}$ (Schleucher, 1998) and $H^{6,\ pro\text{-}S}/H^{6,\ pro\text{-}R}$ (Ehlers et al., 2015) both increase. Such a trend can be easily explained by the contribution of the photorespiration-generated PGA (**2d** in Fig. 2), which has the isotopic compositions of its two C-Hs at C3 ($H^{3,\ pro-S}$ and $H^{3,\ pro-R}$) unequally affected by photorespiration (Ehlers et al., 2015), to the chloroplastic PGA (**2**) pool and the contribution of cellular water (stromal water H_2O and peroxisomal water H_2O) brought about by the exchange opportunities during glucose biosynthesis incorporating the photorespiration-generated PGA (**2d**):

i) the two C-Hs at C1 ($H^{1\alpha}$, the *pro*-R H and $H^{1\beta}$, the *pro*-S H) of RuBP (**1a**) are replaced with chloroplastic water (H_2O) faster than those at C5 during the CBB Cycle (compare RuBP (**1a**) with the three regenerated Ru5Ps **11a**, **11b** and **11c**). Note that the peroxisomal water-derived H in PGA (2d) also ends up in RuBP (1a) after a complete CBB cycle;
ii) no transferable hydrogen of chloroplastic NADPH ever ends up at C1 and C5 of RuBP (**1a** in Fig. 2) (without being significantly exchanged with chloroplastic (stromal) water);
iii) the isotopic composition of the $H^{3,\ pro-R}$ (the blue underlined H of PGA (**2d**), Hanson 1984) is determined by that of the peroxisomal water (H_2O) plus the isotope enrichment associated with the incorporation of peroxisomal water into the *pro*-R position of glycine by the GGT (glutamate-glycine transaminase, Chen and Schirch, 1973), as such it is more enriched in ^2H than $H^{5\alpha}$ (*pro*-R), $H^{5\beta}$ (*pro*-S) and $H^{1\beta}$ (*pro*-S) in RuBP (**1a**). There is an unequal impact of the solvent on $H^{3,\ pro-R}$ and $H^{3,\ pro-S}$ as isotopic composition of the $H^{3,\ pro-S}$ (the $H^{1\beta}$ of PGA (**2d**)) is determined by that of the $H^{1,\ pro-S}$ (the $H^{1\beta}$) of RuBP (**1a**), the KIE_{SHMT} (Chen and Schirch, 1973; Schirch and Jenkins 1964) associated with the abstraction of H^{pro-S} ($H^{1\beta}$) from glycine by SHMT (serine hydroxymethyltransferase) and the glycine-to-serine conversion yield.

When the photorespiration-generated PGA (**2d**) is mixed with the chloroplastic PGA (**2**) pool, the $H^{3,\ pro-S}/H^{3,\ pro-R}$ ratio in PGA (**2d**) changes the $H^{3,\ pro-S}/H^{3,\ pro-R}$ of PGA (**2**) directly, and the $H^{6,\ pro-S}/H^{6,\ pro-R}$ of glucose indirectly in a V_o/V_c-ratio-dependent fashion: **a**) when the V_o/V_c is low, it will be unlikely that the $H^{3,\ pro-S}/H^{3,\ pro-R}$ ratio of PGA (**2**) will change significantly as the contribution of PGA (**2d**) to PGA (**2**) is insignificant, a situation likely to be seen in C_4 photosynthesis; **b**) when the V_o/V_c is high or modest, the glycine-to-serine conversion yield and KIE_{SHMT} are high (fully committed photorespiration), depending on the actual value of the V_o/V_c ratio, the $H^{3,\ pro-S}/H^{3,\ pro-R}$ ratio of PGA (**2**) can be greater than, equal to or smaller than 1, but is still predicted to be positively correlated with the $[O_2]/[CO_2]$ ratio. **c**) when the V_o/V_c is high, conversion yield and KIE_{SHMT} are low (partially committed photorespiration), it is likely that the $H^{3,\ pro-S}/H^{3,\ pro-R}$ ratio of PGA (**2**) decreases and is smaller than 1, but is predicted to be negatively correlated with $[O_2]/[CO_2]$ ratio although the sensitivity to $[O_2]/[CO_2]$ ratio change is low. As a large influx of nitrogen into the peroxisome is needed for the generation of glycine from glyoxylate, this scenario is less likely

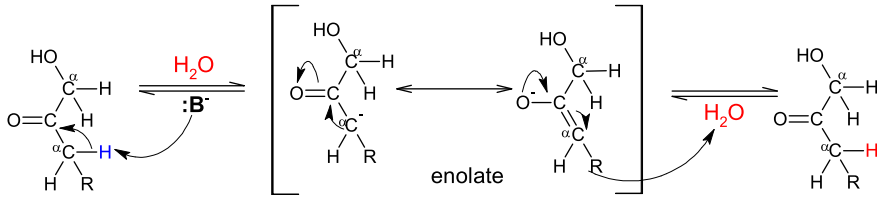

Fig. 5. The exchange of α-H (H^3) in fructose with cellular water. The **B:** represents the negatively charged amino acid residue of the enzyme in a basic medium such as the cytosol and chloroplast.

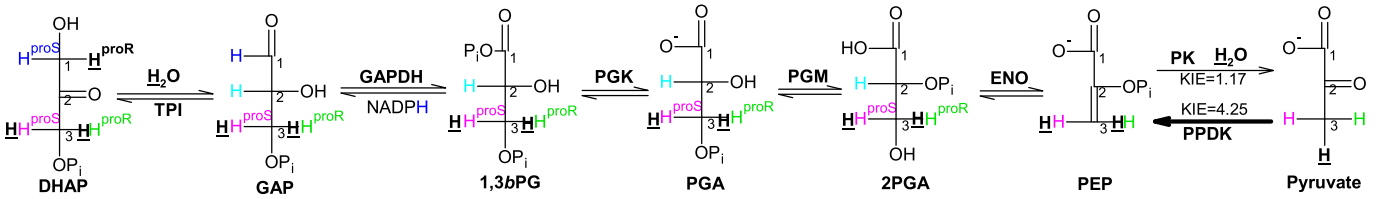

Fig. 6. Mechanisms for labelling of the two Hs at C3 of triose phosphates in the triose phosphates shuttle in NADPH-ME subtype (cf Fig. 4A). Reconstructed metabolic pathways from comparative proteomics studies (Friso et al., 2010) showed that the glycolysis links the malate-oxaloacetate shuttle and the triose-phosphate shuttle via PEP (phosphoenolpyruvate). Conversion of PEP to pyruvate by PK (pyruvate kinase) introduces an M cellular water signal to pyruvate with a slight KIE of 1.17 (Gold and Kessick, 1965). On being converted back to PEP with a KIE as high as 4.85 (Croteau and Wheeler, 1987) and further to GAP and DHAP, the M cellular water signal is preserved in the two prochiral Hs of these two triose phosphates. **H:** hydrogen from cellular water; TPI: triose phosphate isomerase; GAPDH: glyceraldehye phosphate dehydrogenase; PGK: phosphoglycerate kinase: ENO: enolase; PPDK: phosphopyruvate dikinase. The C1, C2 and C3 are structurally equivalent to C_{3C}, C_{24}, and C_{15} in GAP (**4a**) and DHAP (**5a**) in Fig. 2 respectively.

than the first two, although it is not impossible in some physiological circumstances.

The positive correlation between $H^{6,\ pro-S}/H^{6,\ pro-R}$ of glucose and $1/[CO_2]_{atmosphere}$ from controlled grown C_3 plants and archived beet (C_3) over the past century (during which atmospheric CO_2 concentration increased steadily) reported by Ehlers et al. (2015) can be interpreted as a highly committed photorespiration with modest to high photorespiration rate.

iv) The two C-Hs at C3 ($H^{3,\ pro-S}$ and $H^{3,\ pro-R}$) of PGA (**2d**) also end up at C1 and C5 of regenerated Ru5Ps (**11a**, **11b** and **11c**), and on phosphorylation, at RuBP (**1a**). The enrichment signal of these two C-Hs is eventually passed onto the H^1 of glucose (G6P, **8a** in Fig. 2). A high V_o/V_c will lead to a higher contribution of the two C-Hs to the H^1 of glucose, hence a positive correlation between $[O_2]/[CO_2]$ ratio and $H^1/H^{6,\ pro-R}$ as observed by Schleucher (1998).

6. Summary

In this VIEWPOINT, a plausible biochemical explanation is presented for the long-observed but inadequately explained contrasting intramolecular ^2H profiles of C_3 and C_4 sugars. Involvement of ^2H-enriched (transferable H of) NADH associated with photorespiration contributes to the relative ^2H enrichment in H^5 and relative ^2H depletion in H^1 and H^6 (in particular $H^{6,\ proR}$) in C_3 plant glucose. Also, export of (transferable Hs of) NADPH from C_4 mesophyll cells to bundle sheath cells and shuttling of triose-phosphates (PGA and DHAP) between C_4 bundle sheath and mesophyll cells contributes to the relative depletion of H^4 and relative enrichment in H^1 & H^6 (in particular $H^{6,\ proR}$) in C_4 plant glucose, respectively. Finally, incorporation of isotopically relatively less enriched BS cellular water into the H^5 of C_4 glucose contributes to the H^5 depletion while incorporation of isotopically relatively more enriched M cellular water into the H^4 of C_3 glucose contributes to the H^4 enrichment.

The hypotheses employed for the explanation, although qualitative in nature, can be tested at least semi-quantitatively by well-designed growth experiments. For example, the contribution of relatively enriched ^2H from NADH to the relative enrichment of H^5 (and H^4) in C_3 plant glucose can easily be tested by growing C_3 plants where environmental conditions are manipulated to enhance or suppress photorespiration. The hypotheses can also be tested on C_3 mutants deficient in photorespiratory enzymes. The hypothesis that the malate-pyruvate shuttle in C_4 plants depletes ^2H of the exported NADPH transferable H and enriches ^2H of the transferable H of the residual NADPH can be tested with C_3-C_4 hybrid plants such as *Flaveria*. In addition to testing these hypotheses, efforts can be made toward building a mathematical model to account for the intramolecular ^2H distribution in C_3 (conceptually similar to the one for intramolecular ^{13}C distribution as developed by Tcherkez et al. (2004)) and C_4 plant glucoses and the differences between them. Such a model would provide quantitative understanding of how isotopically discriminating biochemical reactions and the metabolites-cellular water isotopic exchanges contribute to the ^2H distribution profiles.

Acknowledgements

YZ was supported by a Shaanxi Provincial Talent 100 Fellowship, a Chinese Natural Science Foundation grant (NSFC 41773032) and a Shaanxi Department of Education grant (17JS013). KG was supported by the ARC Discovery Project series (DP130100577 and DP1096729). GDF & AG were supported by the Alexander-von-Humboldt foundation (Humboldt Research Award to GDF). The helpful discussion with Prof Robert Furbank on NADP-ME metabolism is gratefully acknowledged. Communications with Prof Guillaume Tcherkez and comments from a few anonymous colleagues greatly improved the manuscript. We thank Phytochemistry editor-in-chief Dr Richard Robins for very helpful comments and excellent editorial assistance in the process of publishing our work.

References

Augusti, A., 2007. Monitoring Climate and Plant Physiology Using Deuterium Isotopomers of Carbohydrates. PhD thesis. Umeå University, Sweden.

Augusti, A., Betson, T.R., Schleucher, J., 2006. Hydrogen exchange during cellulose synthesis distinguishes climatic and biochemical isotope fractionations in tree

rings. New Phytol. 172, 490–499.
Augusti, A., Betson, T.R., Schleucher, J., 2008. Deriving correlated climate and physiological signals from deuterium isotopomers in tree rings. Chem. Geol. 252, 1–8.
baz Jackson, J., Peake, S.J., White, J.A., 1999. Structure and mechanism of proton-translocating transhydrogenase. FEBS Lett. 4, 1–8.
Betson, T.R., Augusti, A., Schleucher, J., 2006. Quantification of deuterium isotopomers of tree-ring cellulose using Nuclear Magnetic Resonance. Anal. Chem. 78, 8406–8411.
Billault, I., Guiet, S., Mabon, F., Robins, R.J., 2001. Natural deuterium distribution in long-chain fatty acids is non-statistical: a site-specific study by quantitative ^{2}H NMR spectroscopy. ChemBioChem 2, 425–431.
Bizouarn, T., Grimley, R.L., Cotton, N.P.J., Stilwell, S.N., Hutton, M., Baz Jackson, J., 1995. The involvement of NADP(H) binding and release in energy transduction by proton-translocating nicotinamide nucleotide transhydrogenase from *Escherichia coli*. Biochimica Biophysica Acta 1229, 49–58.
Canellas, P.F., Cleland, W.W., 1991. Carbon-13 and deuterium effects on the reaction catalyzed by glyceraldehyde-3-phosphate dehydrogenase. Biochemistry 30, 8871–8876.
Chen, M.S., Schirch, L.V., 1973. Serine transhydroxymethylase. J. Biol. Chem. 248, 7979–7984.
Cook, P.F., Blanchard, J.S., Cleland, W.W., 1980. Primary and secondary deuterium isotope effects on equilibrium constants for enzyme-catalyzed reactions. Biochemistry 19, 4853–4858.
Croteau, R.B., Wheeler, C.J., 1987. Isotopically sensitive branching in the formation of cyclic monoterpenes: proof that (-)-α-pines and (-)-β-pinene are synthesized by the same monoterpene cyclase via deprotonation of a common intermediate. Biochemistry 26, 5383–5389.
Dellero, Y., Mauve, C., Boex-Fontvielle, E., Flesch, V., Jossier, M., Tcherkez, G., Hodges, M., 2015. Experimental evidence for a hydride transfer mechanism in plant glycolate oxidase catalysis. J. Biol. Chem. 290, 1689–1698.
Edwards, G.E., Walker, D.A., 1983. C_3, C_4: Mechanisms, and Cellular and Environmental Regulation of Photosynthesis. Blackwell Scientific, Oxford, p. 542.
Edwards, G.E., Voznesenskaya, E.V., 2011. C_4 photosynthesis: Kranz forms and single-cell C_4 in terrestrial plants. In: Raghavendra, A.S., Sage, R.F. (Eds.), C_4 Photosynthesis and Related CO_2 Concentrating Mechanisms. Advances in Photosynthesis and Respiration, Vol. 32. Springer, Dordrecht, The Netherlands, pp. 29–61.
Ehlers, I., August, A., Beston, T.R., Nilson, M.B., Marshall, J.D., Schleucher, J., 2015. Detecting long-term metabolic shifts using isotopomers: CO_2-driven suppression of photorespiration in C_3 plants over the 20th century. Proc. Natl. Acad. Sci. U. S. A. 112, 15585–15590.
Friso, G., Majeran, W., Huang, M.S., Sun, Q., van Wijk, K.J., 2010. Reconstruction of metabolic pathways, protein expression, and homeostasis machineries across maize bundle sheath and mesophyll chloroplasts: large-scale quantitative proteomics using the first maize genome assembly. Plant Physiol. 152, 1219–1250.
Gilbert, A., Silvestre, V., Robins, R.J., Remaud, G.S., Tcherkez, G., 2012. Biochemical and physiological determinants of intramolecular isotope patterns in sucrose from C_3, C_4 and CAM plants accessed by isotopic ^{13}C NMR spectrometry: a viewpoint. Nat. Product. Rep. 29, 476–486.
Gleixner, G., Schmidt, H.-L., 1997. Carbon isotope effects on the fructose-1,6-*bis*phosphate aldolase reaction, origin for non-statistical ^{13}C distributions in carbohydrates. J. Biol. Chem. 272, 5382–5387.
Gold, V., Kessick, M.A., 1965. Hydrogen isotope effects in olefin hydration. The relationship of isotope effects to the mechanism of proton transfer from the hydronium ion. J. Chem. Soc. 10, 6718–6729.
Grice, K., Lu, H., Zhou, Y.P., Stuart-Williams, H., Farquhar, G.D., 2008. Biosynthetic and environmental effects on the stable carbon isotopic compositions of *ante-iso*- (3-methyl) and *iso*- (2-methyl) alkanes in tobacco leaves. Phytochemistry 69, 2807–2814.
Grissom, C.B., Cleland, W.W., 1985. Use of intermediate partitioning to calculate intrinsic isotope effects for the reaction catalyzed by malic enzyme. Biochemistry 24, 944–948.
Hanson, K.R., 1984. Stereochemical determination of carbon partitioning between photosynthesis and photorespiration in C_3 plants: use of (3*R*)-D-[3-$^{3}H_1$, 3-^{14}C] glyceric acid. Archives Biochem. Biophysics 232, 58–75.
Heldt, H.-W., 2005. Plant Biochemistry, an update and translation of the German, third ed. Elsevier. Academic Press, pp. 235–240.
Hermes, J.D., Roeske, C.A., O'Leary, M.H., Cleland, W.W., 1982. Use of multiple isotope effects to determine enzyme mechanisms and intrinsic isotope effects. Malic enzyme and glucose-6-phosphate dehydrogenase. Biochemistry 21, 5106–5114.
Ishimaru, K., Ohkawa, Y., Shige, T., Tobias, D.J., Ohsugi, R., 1998. Elevated pyruvate, orthophosphate dikinase (PPDK) activity alters carbon metabolism in C_3 transgenic potatoes with a C_4 maize PPDK gene. Physiol. Plantarum 103, 340–346.
Jordan, P.M., Akhtar, M., 1970. The mechanism of action of serine transhydroxymethylase. Biochem. J. 116, 277–286.
Kawashima, N., Mitake, T., 1969. Studies on protein metabolism in higher plants. J. Agric. Biol. Chem. 3, 539–543.
Keister, D.L., san Pietro, Stolzenbach, F.E., 1960. Pyridine nucleotide transhydrogenase from spinach. J. Biol. Chem. 235, 2989–2996.
Liu, X., An, W., Treydte, K., Wang, W., Xu, G., Zeng, X., Wu, G., Wang, B., Zhang, X., 2015. Pooled versus separate tree-ring δD measurements, and implications for reconstruction of the Arctic Oscillation in northwestern China. Sci. Total Environ. 511, 584–594.
Luo, Y.H., Sternberg, L., 1991. Deuterium heterogeneity in starch and cellulose nitrate of CAM and C_3 plants. Phytochemistry 30, 1095–1098.
Luo, Y.H., Sternberg, L., Suda, S., Kumazawa, S., Mitsui, A., 1991. Extremely low D/H ratios of photoproduced hydrogen by cyanobacteria. Plant Cell Physiol. 32, 897–900.
Majeran, W., Cai, Y., Sun, Q., van Wijk, K.J., 2005. Functional differentiation of bundle sheath and mesophyll maize chloroplasts determined by comparative proteomics. Plant Cell 17, 3111–3140.
Martin, G.J., Martin, M.L., 1981. Deuterium labelling at the natural abundance level as studied by high field quantitative ^{2}H NMR. Tetrahedron Lett. 22, 3525–3528.
Martin, M.L., Martin, G.J., 1991. Deuterium NMR in the study of site-specific natural isotope fractionation (SNIF-NMR). In: Diehl, P., Fluck, E., Günther, H., Kosfeld, R., Seelig, J. (Eds.), NMR Basic Principles and Progress, vol. 23. Springer Verlag, Berlin, pp. 1–61.
Miller, R.T., Hinck, A.P., 2001. Characterization of hydride transfer to flavine adenine dinucleotide in neuronal nitric oxide synthase reductions domain: geometric relationship between the nicotinamide and isoalloxazine rings. Archives Biochem. Biophysics 395, 129–135.
Niedermeyer, E.M., Forrest, M., Beckmann, B., Sessions, A.L., Mulch, A., Schefuß, E., 2016. The stable hydrogen isotopic composition of sedimentary plant waxes as quantitative proxy for rainfall in the West African Sahel. Geochim. Cosmochim. Acta 184, 55–70.
O'Donoghue, A.C., Amyes, T.L., Richard, J.P., 2005a. Hydron transfer catalyzed by triosephosphate isomerase. Products of isomerization of (R)-glyceraldehyde 3-phosphate in D_2O. Biochemistry 44, 2610–2621.
O'Donoghue, A.C., Amyes, T.L., Richard, J.P., 2005b. Hydron transfer catalyzed by triosephosphate isomerase. Products of isomerization of dihydroxyacetone phosphate in D_2O. Biochemistry 44, 2622–2631.
Pionnier, S., Zhang, B.-L., 2002. Application of ^{2}H NMR to the study of natural site-specific hydrogen isotope transfer among substrate, medium, and glycerol in glucose fermentation with yeast. Anal. Biochem. 307, 138–146.
Pionnier, S., Robin, R.J., Zhang, B.-L., 2003. Natural abundance hydrogen isotope affiliation between the reactants and the products in glucose fermentation with yeast. J. Agric. Food Chem. 51, 2076–2082.
Robins, R.J., Billault, I., Duan, J.-R., Guiet, S., Pionnier, S., Zhang, B.-L., 2003. Measurements of ^{2}H distribution in natural products by quantitative ^{2}H NMR: an approach to understanding metabolism and enzyme mechanism. Phytochem. Rev. 2, 87–102.
Robins, J.R., Pétavy, F., Nemmaoui, Y., Ayadi, F., Silvestre, V., Zhang, B.-L., 2008. Non-equivalence of hydrogen transfer from glucose to the *pro*-R and *pro*-S methylene positions of ethanol during fermentation by *Leuconostoc mesenteroides* quantified by ^{2}H NMR at natural abundance. J. Biol. Chem. 283, 19704–19712.
Shirch, L.V., Jenkins, W.T., 1964. Serine transhydroxymethylase. Properties of the enzyme-substrate complexes of D-alanine and glycine. J. Biol. Chem. 239 (11), 3801–3807.
Schleucher, J., 1998. Intramolecular deuterium distribution and plant growth conditions. In: Griffith, H. (Ed.), Stable Isotopes, Integration of Biological, Ecological and Geochemical Processes. BIOS Scientific Publishers Ltd., Oxford, pp. 63–73.
Schleucher, J., Vanderveer, P.J., Sharkey, T.D., 1998. Export of carbon from chloroplasts at night. Plant Physiol. 118, 1439–1445.
Schleucher, J., Vanderveer, P., Markley, J.L., Sharkey, T.D., 1999. Intramolecular deuterium distribution reveals disequilibrium of chloroplast phosphoglucose isomerase. Plant, Cell Environ. 22, 525–533.
Schmidt, H.-L., Werner, R., Eisenreich, W., 2003. Systematics of ^{2}H patterns of natural compounds and its importance for the elucidation of biosynthetic pathways. Phytochem. Rev. 2, 61–85.
Sessions, A.L., Burgoyne, T.W., Schimmelmann, A., Hayes, J.M., 1999. Fractionation of hydrogen isotopes in lipid biosynthesis. Org. Geochem. 30, 1193–1200.
Siegel, M.I., Wishnick, M., Lane, M.D., 1972. Ribulose-1,5-diphosphate carboxylase. In: Boyer, P.D. (Ed.), Carboxylation and Decarboxylation (Non-oxidative Isomerisation), third ed. Academic Press, NY & London.
Smith, B.N., Ziegler, H., Lipp, J., 1991. Isotopic evidence for mesophyll reduction in *Zea mays*, an NADP-malic enzyme plant. Naturwissenschaften 78, 358–359.
Sternberg, L., de Niro, M.J., Johnson, H.B., 1986. Oxygen and hydrogen isotope ratios of water from photosynthetic tissues of CAM and C_3 plants. Plant Physiol. 82, 428–431.
Taiz, Zeiger, 2006. Photosynthesis: carbon reactions. In: Plant Physiology, fourth ed. Sinauer Associates, Sunderland, USA, pp. 159–195.
Tcherkez, G., 2010. Isotopie biologique: Introduction aux effets isotopiques et à leurs applications en biologie. Éditions Tec et Doc/Lavoisier, pp. 170–175.
Tcherkez, G., Farquhar, G.D., Beadeck, F., Ghashghaie, J., 2004. Theoretical considertions about carbon isotope distribution in glucose C_3 plants. Funct. Plant Biol. 3, 857–877.
Tcherkez, G.G., Bathellier, C., Stuart-Williams, H., Whitney, S., Gout, E., Bligny, R., Badger, M., Farquhar, G.D., 2013. D_2O solvent isotope effects suggest uniform energy barriers in ribulose-1,5-bisphosphate carboxylase/oxygenase catalysis. Biochemistry 52, 869–877.
von Caemmerer, S., Furbank, R.T., 2016. Strategies for improving C4 photosynthesis. Curr. Opin. Plant Biol. 31, 125–134.
Yakir, D., 1992. Variations in the natural abundance of oxygen-18 and deuterium in plant carbohydrates. Plant, Cell Environ. 15, 1005–1020.
Zhang, B.L., Quemerais, B., Martin, M.L., Martin, G.J., Williams, J.M., 1994. Determination of the natural deuterium distribution in glucose from plants having

different photosynthetic pathways. Phytochem. Anal. 5, 105–110.
Zhang, B.L., Billault, I., Li, X.B., Mabon, F., Remaud, G., Martin, M.L., 2002. Hydrogen isotopic profile in the characterization of sugars. Influence of the metabolic pathway. J. Agric. Food Chem. 50, 1574–1580.
Zhang, X.N., Gillespie, A., Sessions, A.L., 2009. Large D/H variations in bacterial lipids reflect central metabolic pathways. Proc. Natl. Acad. Sci. U. S. A. 106, 12580–12586.
Zhou, Y.P., Grice, K., Stuart-Williams, H., Farquhar, G.D., Hocart, C., Lu, H., Liu, W.G., 2010. Biosynthetic origin of the saw-toothed profile in $\delta^{13}C$ and $\delta^{2}H$ of *n*-alkanes and systematic isotopic differences between *n*-, *iso*- & *anteiso*-alkanes in leaf waxes of land plants. Phytochemistry 71, 388–403.
Zhou, Y.P., Grice, K., Chikaraishi, Y., Stuart-Williams, H., Farquhar, G.D., Ohkouchi, N., 2011. Temperature effect on leaf water deuterium enrichment and isotopic fractionation during leaf lipid biosynthesis: results from controlled growth of C_3 and C_4 land plants. Phytochemistry 72, 207–213.
Zhou, Y.P., Stuart-Williams, H., Grice, K., Kayler, Z.E., Zavadlav, S., Gessler, A., Farquhar, G.D., 2015. Allocate carbon for a reason: priorities are reflected in the $^{13}C/^{12}C$ ratios of plant lipids synthesized via three independent biosynthetic pathways. Phytochemistry 111, 14–20.
Zhou, Y.P., Grice, K., Stuart-Williams, H., Hocart, C.H., Gessler, A., Farquhar, G.D., 2016. Hydrogen isotopic differences between C_3 and C_4 land plant lipids: consequences of compartmentation in C_4 photosynthetic chemistry and C_3 photorespiration. Plant, Cell Environ. 39, 2676–2690.